

New 2×2 and 1×3 Multimode Interference Couplers with Free Selection of Power Splitting Ratios

Pierre A. Besse, Emilio Gini, Maurus Bachmann, and Hans Melchior, *Fellow, IEEE*

Abstract—We report on the concept and realization of new 2×2 and 1×3 multimode interference (MMI) couplers that offer the possibility of a free choice of the power splitting ratio. These MMI devices, using a new butterfly geometrical design, are compact, polarization-insensitive, and tolerant to fabrication parameters. Realized in InGaAsP/InP with large fabrication tolerances, they permit the control of the output powers within a few percentage points for both polarizations. The measurement results fit well the theoretical predictions. Extensions of the design are presented that assure a fully symmetrical geometry and therefore an optimal homogeneity of the device characteristics. Based on the same idea, a new compact mode converter-combiner is proposed.

I. INTRODUCTION

POWER SPLITTING is a basic function of the integrated optics. Such devices play a central role in passive optical distribution networks, in complex photonic integrated circuits, as well as in advanced active optical components such as interferometers, switches [1], [2], and nonlinear all-optical devices [3], [4]. Various solutions have been proposed and realized to split or to combine optical signals. Especially, in the last few years, multimode interference (MMI)-couplers [5], [6] have demonstrated attractive properties [7]–[10]. They are compact, tolerant to the fabrication parameters, and polarization-independent when strongly guided structures are used [11]. By using the standard rectangular geometrical design of the multimode waveguide section [12], only discrete values of the splitting ratios can be obtained even when an overlapping of the self images is introduced [10], [13].

For several applications, MMI-couplers with free choice of the splitting ratio would be highly advantageous. In networks, the “tap” function requires only a small part of the light to be extracted from an optical channel. Furthermore, the exact quantity of extracted light has to be adapted to each situation. In ring lasers, where 2×2 MMI couplers have successfully been introduced [14] as outcoupling elements, the splitting ratio of the MMI element influences the characteristics of the entire device. In fact, in ring lasers, a change of the transmission of the coupler corresponds to a variation of the facet reflectivities in a straight laser waveguide. A free choice

of the splitting ratio is also advantageous in Mach–Zehnder interferometers (MZI) when losses or gain are asymmetrically distributed between both arms of the device. This effect can be compensated by introducing an inverse asymmetry in the splitting ratio in order to restore a maximum contrast of the interference fringes [15].

In [16] a new class of MMI couplers that rely on especially shaped interference sections have been presented to achieve freely chosen splitting ratios. The concept of Butterfly MMI couplers has been introduced. In this paper, we expose in details this concept and apply it to new devices like fully symmetrized 2×2 splitters, 1×3 splitters and mode converter-combiners. In Section II the concept of Butterfly MMI couplers is developed after [16]. By transforming the rectangular geometry of standard MMI devices into a series of down- and up-tapered profiles, ultra-compact phase shifters are introduced in the components. The splitting ratios are then a simple function of the taper parameters and can be adapted from device to device.

In Section III, we apply the Butterfly concept to 2×2 power splitters. This section resumes the results of [16] in order to give an introduction to the new devices of Sections IV, V, and VI. We first choose four 2×2 couplers having rectangular MMI sections and four different discrete values of the splitting ratios [13]. The new butterfly geometry is then introduced in these four basic elements. These four kinds of devices together cover the entire range of possible ratios for 2×2 power splitters. These new 2×2 coupler structures have been realized in InGaAsP/InP. The output powers are polarization-independent and accurate to within a few percentage points [16].

In Section IV, the butterfly concept is applied to 1×3 power splitters. Two kinds of new devices are developed that permit a free choice of the light intensity in the central output compared to the light equally split to the outer channels. Again, these devices have been realized in InGaAsP/InP where polarization independency and accuracy within a few percentage points have been measured.

In Section V, generalizations of the butterfly configuration are presented. First we replace two of the asymmetrical devices used in Section III and IV by new elements with a fully symmetrical geometry, but with multiple tapered sections. The symmetrical behavior assures an optimal homogeneity of the device characteristics. Another generalization leads to the development of a new compact mode converter-combiner. This device images the fundamental mode of an input to

Manuscript received October 5, 1995; revised July 1, 1996.

P. A. Besse was with the Institute of Quantum Electronics, ETH-Zurich, Switzerland. He is now with the Department of Microengineering, EPFL Lausanne, Switzerland.

E. Gini and H. Melchior are with the Institute of Quantum Electronics, ETH-Zurich, Switzerland.

M. Bachmann was with the Institute of Quantum Electronics, ETH-Zurich, Switzerland. He is now with Alcatel Alsthom Recherche, Marcoussi, France.

Publisher Item Identifier S 0733-8724(96)07654-2.

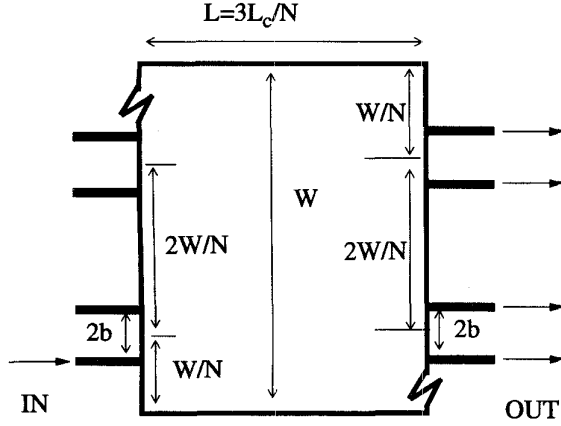


Fig. 1. General design of conventional MMI couplers after [12]. A proper choice of the waveguide separation parameter b leads to overlapping self-images in the outputs. Especially following four 2×2 couplers with discrete splitting ratios P_c/P_b are obtained for symmetrical input modes: Basic device "A": $N = 6, b = W/6, P_c/P_b = 50/50$, Basic device "B": $N = 3, b = 0, P_c/P_b = 100/0$, Basic device "C": $N = 4, b = 0, P_c/P_b \cong 85/15$, Basic device "D": $N = 5, b = 0, P_c/P_b \cong 72/28$.

the fundamental mode of the output and at the same time it converts the fundamental mode of a second input to the first order mode of the same output. This element has basically the same functionality as passive adiabatic asymmetric Y-junctions [17].

In the last section, different applications of the new butterfly MMI couplers are proposed and analyzed. In particular, new designs of ring-lasers and MZI are developed. Furthermore, 1×3 Butterfly MMI couplers can be used as multifunctional devices in optical interferometers to perform at the same time the tap- and splitter-function.

II. CONCEPTS AND DESIGN PRINCIPLES

In this section, we expose in details the concept of Butterfly MMI couplers as introduced in [16]. We first briefly summarize the design of the conventional MMI elements with rectangular multimode section.

A. Standard Devices with a Conventional Rectangular MMI Section

The general design of MMI couplers is shown in Fig. 1. For a device length $L = 3L_c/N$, N self images of the same intensity appear at the outputs [12]. Every input is self-imaged to every output. The coupling length L_c is approximately given by

$$L_c \cong \frac{4}{3}n \cdot \frac{W^2}{\lambda} \quad (1)$$

with n the effective refractive index and W the effective width of the MMI section and λ the wavelength. For lateral strong guided structures, the effective width W corresponds well to the geometrical width of the multimode section. In general, the waveguide separation parameter b , determining the locations of the inputs and outputs, can be freely chosen. Homogeneous power splitting is obtained for values of b that lead to well separated outputs, the devices will then act as $N \times N$ -couplers.

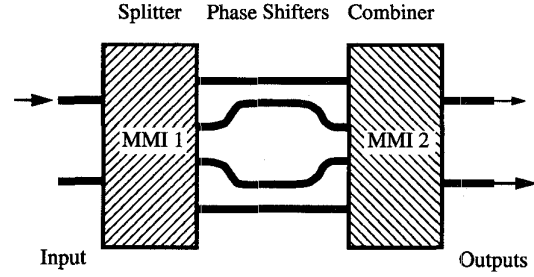


Fig. 2. Principle of operation of the MMI couplers with a free selection of the splitting ratios. The couplers are cut into two sections called MMI 1 and MMI 2. Phase shifters are introduced between these sections. Ultra-compact phase shifters can be obtained using the new butterfly geometry. The whole device acts as a multileg MZI.

By choosing $b = 0$ or $b = W/N$, overlapping of the self-images occurs [13]. Due to interference effects, a wide range of special MMI couplers can be identified. Some of them, the symmetric interference $1 \times N$ -couplers and the restricted interference $2 \times N$ -couplers, have homogeneous splitting ratios at the outputs, but in general the interference process results in well defined, discrete nonuniform values of the splitting ratios. For example, in the case of 2×2 couplers with a rectangular geometry, the following four discrete values of the ratio P_c/P_b can be realized [13]

$$\frac{P_c}{P_b} \cong \left\{ \frac{50}{50}, \frac{100}{0}, \frac{85}{15}, \frac{72}{28} \right\}. \quad (2)$$

The inverse ratios can also be obtained by adding a cross-coupler to the devices, but other ratios are impossible to be realized with conventional MMI couplers.

B. Concept of the Butterfly Geometrical Configuration

In order to vary these splitting ratios, we have developed in [16] a specific geometrical design of the MMI couplers. The principle of operation is explained in Fig. 2. The coupler is cut in two or in many sections, and phase shifters are introduced between them. It results in multileg MZI's [18]. The splitting ratios can be chosen by adapting the phase shifts.

For a practical realization, the phase shifters have to be accurate and ultra-compact. We therefore introduce the butterfly geometrical configuration (Fig. 3) [16]. The two sections are transformed in a linearly down-tapered and a linearly up-tapered section, respectively. By this transformation the self-imaging properties remain [19]. We suppose that strong lateral guiding is assured all along the device. The expression of L in terms of L_c is unchanged but L_c should now be expressed as

$$L_c \cong \frac{4}{3}n \cdot \frac{(W_0 \cdot W_1)}{\lambda} \quad (3)$$

where W_0 and W_1 represent the effective widths of the MMI section at the input and in the center, respectively. The inputs and outputs of both MMI sections are located on concentric circles. In the center, the light has to propagate from O_0 to I_1 . This propagation is laterally not guided but the propagation distance remains less than a few wavelengths. The distance

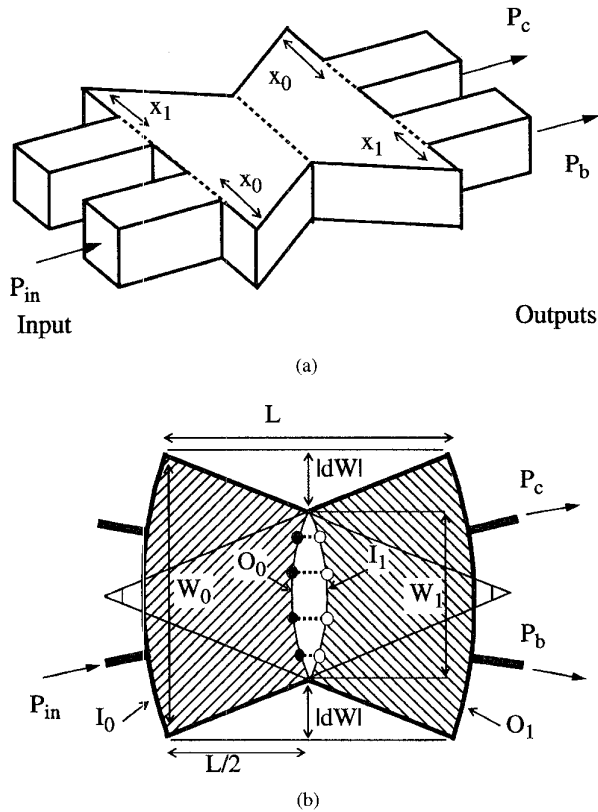


Fig. 3. Principle of the geometrical design of the "butterfly" MMI couplers after [16]. The MMI couplers are divided into a linearly down-tapered and a linearly up-tapered section. By adapting the length of each section according to (3), the self-imaging properties remain. The images after the first section (represented by full circles) are located on the curve O_0 , but the inputs of the second section (represented by open circles) are located on the curve I_1 . The distance between O_0 and I_1 corresponds to a phase shift and depends on the lateral position of the different images. These relative phase differences, accurately controlled by the parameter dW , influence the power splitting ratio of the whole device.

between the two curves O_0 to I_1 leads to the introduction of phase differences between both MMI sections [20]. They can accurately be controlled by the width variation dW .

The geometrical configuration has to be adapted to obtain the required phase shifts between the two tapered sections. Fig. 3 presents a symmetrical decrease of the width of the MMI device. In Fig. 4(a) the phase shifts are obtained with a symmetrical increase of the width of the MMI coupler, while in Fig. 4(b) an asymmetric width variation is applied. The study of these cases is analog to the first one.

III. 2×2 POWER SPLITTERS

In this section, we summarize the results of [16], where the Butterfly configuration was applied on 2×2 power splitters. We take four 2×2 couplers having rectangular MMI sections, apply the butterfly geometry on these components, and obtain devices that cover the entire range of possible ratios for 2×2 power splitters. Devices, realized in InGaAsP/InP, show a good polarization independency and an accuracy within a few percents.

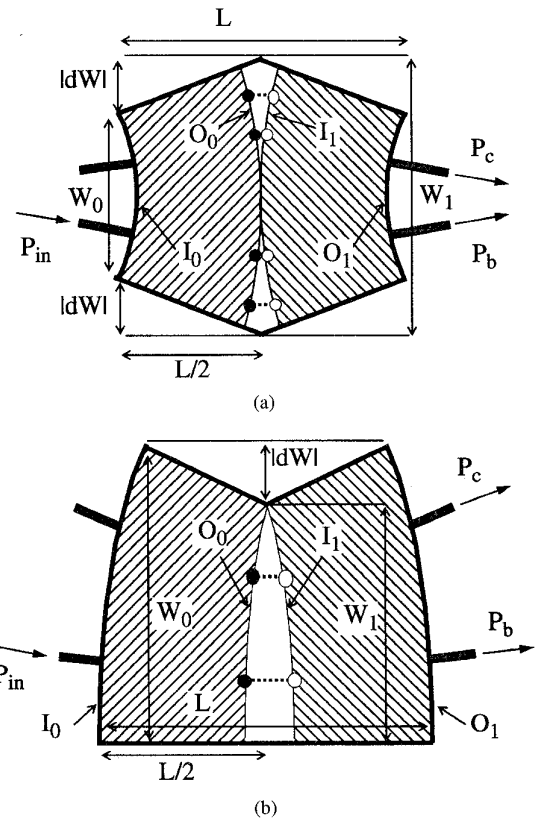


Fig. 4. Alternatives to the geometrical design of the "butterfly" MMI couplers [16]. The principle is the same as in Fig. 3, but different phase changes are obtained in order to influence the power splitting ratio: (a) symmetric butterfly configuration with increasing width, and (b) asymmetric butterfly configuration with width variation only on one side.

A. Design of 2×2 Butterfly MMI Couplers

Using conventional rectangular sections, 2×2 MMI couplers with four different discrete splitting ratios P_c/P_b can be obtained (Fig. 1). The devices (named basic "A" and "B") of length $L_c/2$ and L_c give the splitting ratios $P_c/P_b = 50/50$ and $100/0$. Two other devices (named basic "C" and "D") using a conventional rectangular MMI section have, respectively, the asymmetric splitting ratios $P_c/P_b \cong 85/15$ and $\cong 72/28$. Their lengths are $3L_c/4$ and $3L_c/5$ respectively. The access waveguides are located at $x_0 = x_1 = W_0/3$, at $x_0 = x_1 = W_0/3$, at $x_0 = x_1 = W_0/4$, and at $x_0 = x_1/2 = W_0/5$ for the devices "A", "B", "C" and "D," respectively.

Applying the butterfly geometry described in the previous section to these four basic devices ("A" to "D"), specific couplers will be obtained that permit the free variation of the splitting ratio as function of a geometrical parameter. For the devices "A," "C," and "D," a symmetric butterfly-configuration, as in Fig. 3 or 4(a), leads to variable splitting ratios. For the device "B" variations are obtained with the asymmetric butterfly-configuration of Fig. 4(b). The splitting ratios can be evaluated by calculating the geometrical path differences between O_0 and I_1 as function of the normalized width variation $d\Omega$. These path differences are then converted in phase shifts and introduced in the theory of multileg MZI

TABLE I
DIMENSIONS OF THE NEW MMI-DEVICES WITHOUT WIDTH
VARIATION. THE DEVICES ARE DESIGNED TO WORK AT
 $\lambda = 1.53\mu\text{m}$ USING THE WAVEGUIDE STRUCTURE OF [16]

	"A"	"B"	"C"	"D"	"I"	"II"
W_0	18	18	12	15	24	24
Length	460	920	308	384	612	1224

[21], [22]. One gets

$$P_c \cong \cos^2(0,5 \cdot \pi \cdot d\Omega)$$

for the devices "A," "B" and "C"

and

$$P_c \cong 0,2 + 0,8 \cdot \cos^2(0,563 \cdot \pi \cdot d\Omega)$$

for the devices "D." (4)

In every case P_b is given by $P_b = 1 - P_c$. The normalized width variation $d\Omega$ is expressed as

$$d\Omega = -\left(\frac{dW}{W_0}\right) - \frac{1}{2} \quad \text{for the devices "A,"}$$

$$d\Omega = \left(\frac{dW}{W_0}\right) \quad \text{for the devices "B,"}$$

$$d\Omega = -\frac{1}{2}\left(\frac{dW}{W_0}\right) - \frac{1}{4} \quad \text{for the devices "C"}$$

and

$$d\Omega = -0,71\left(\frac{dW}{W_0}\right) - 0,355 \quad \text{for the devices "D." (5)}$$

B. Experimental Results on 2×2 Butterfly MMI Couplers

Experimentally, the condition of a strong lateral guiding together with the requirement of a compact device limit the possible range of width variations, so that one device type cant cover the whole range of splitting ratio. However, by properly choosing among the four device types, any ratio can be obtained with realistic width variations. Note that each device has two possible inputs and the ratios P_c/P_b between 50/50 and 0/100 can be obtained by interchanging the input position or by adding a cross-coupler to the devices.

For the realization of the butterfly MMI couplers we use the same structure [16] as for our polarization independent switches [2]. The effective widths W_0 for the TE polarization and the lengths L for $dW = 0$ are listed in Table I. The maximal width variations ($W_1 - W_0$) are $\pm 4 \mu\text{m}$. The devices have been measured at $\lambda = 1.53 \mu\text{m}$ (Fig. 5). Any splitting ratio can be realized and the devices are polarization insensitive. The excess-losses, compared to a straight waveguide, remain lower than 0.7 dB [16].

IV. NEW 1×3 POWER SPLITTERS

A. Design of 1×3 Butterfly MMI Couplers

As for the 2×2 splitters, we first chose basic 1×3 structures with rectangular geometry. The basic device named "I" has $L = 3L_c/8$, $N = 8$ and $b = W/8$ (Fig. 1). The basic device

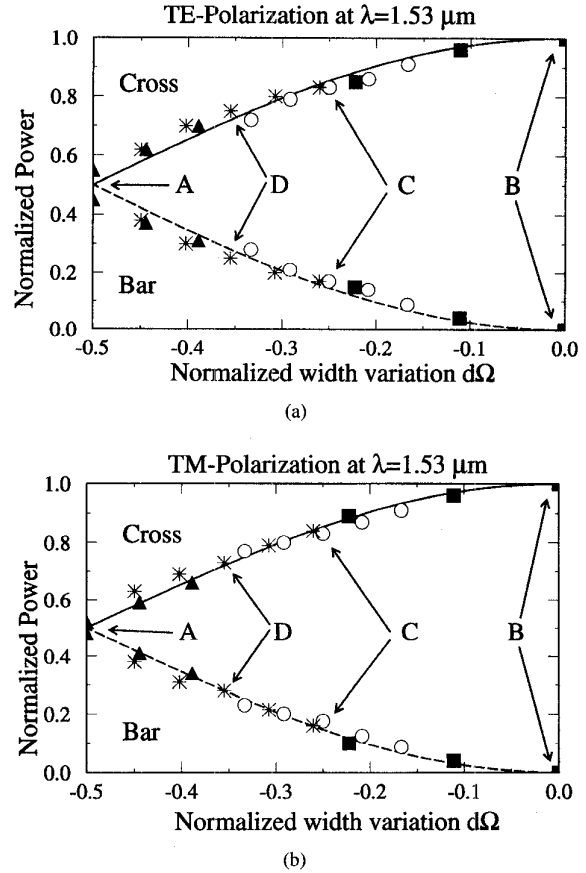


Fig. 5. Measured power splitting ratios at $\lambda = 1.53\mu\text{m}$ of the 2×2 "butterfly" MMI couplers (after [16]) as a function of the normalized width variation $d\Omega$ as defined in the text. The excess-losses remain lower than 0.7 dB. By choosing one of the devices "A" (full triangles), "B" (full boxes), "C" (open circles), and "D" (asterisk) the output powers P_c and P_b can be accurately selected within a few percentage points. The solid and dashed lines correspond to the theoretical calculations for P_c , respectively, P_b for the "butterfly" devices, "A," "B," and "C" (4). They are identical in both figures, showing the good polarization insensitivity of the fabricated devices.

named "II" has $L = 3L_c/4$, $N = 4$ and $b = W/4$. For both devices, the input and one output are centered, the two other outputs being at $W/4$ from each side. The symmetrical butterfly configuration of Fig. 3 and the asymmetrical configuration of Fig. 4(b) are applied, respectively, to the devices "I" and "II" in order to permit a free choice of the light intensity in the central output compared to the light equally split to the outer channels. A schematic view of these elements are shown in the insert of Fig. 6. Again, the splitting ratios can be evaluated by calculating the geometrical path differences between O_0 and I_1 as function of the normalized width variation $d\Omega$. One gets

$$P_2 \cong \sin^2(\pi \cdot d\Omega) \quad \text{for both the devices "I" and "II." (6)}$$

In every case P_1 and P_3 are given by $P_1 = P_3 = (1 - P_2)/2$. The normalized width variation $d\Omega$ is expressed as

$$d\Omega = \left(\frac{dW}{W_0}\right) \quad \text{for the devices "I"}$$

and

$$d\Omega = -\left(\frac{dW}{W_0}\right) - \frac{1}{2} \quad \text{for the devices "II." (7)}$$

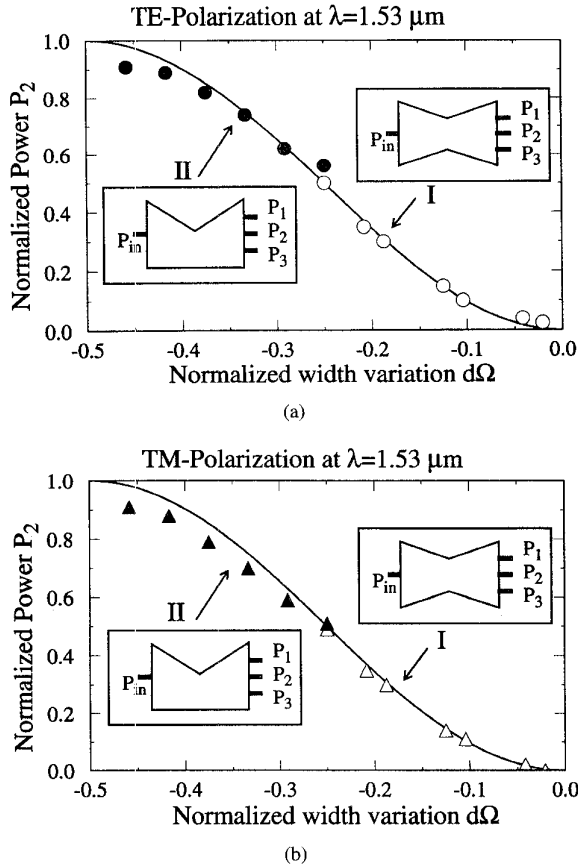


Fig. 6. Measured power splitting ratios at $\lambda = 1.53 \mu\text{m}$ of the new 1×3 "butterfly" MMI couplers as function of the normalized width variation $d\Omega$ as defined in the text. The waveguide structure is given in [16]. The excess-losses remain lower than 1.0 dB. By choosing one of the new devices "I" (open symbols) and "II" (full symbols) the output powers P_2 and $P_1 = P_3$ can be accurately selected within a few percent. The devices "I" and "II" are drawn in insert. The solid and dashed lines correspond to the theoretical calculations (6). They are identical in both figures, showing the good polarization insensitivity of the fabricated devices.

Note that two other devices, working as 2×3 splitters, lead to the light distribution: $P_1 \approx 1/8, P_2 = P_3 \approx 7/16$. The first device, named "III," has $L = 3L_c/6, N = 6$ and $b = 0$ (Fig. 1) and the geometrical configuration of Fig. 4(a) with $W_1/W_0 \approx 1.37$. The inputs are located at $W_0/6$ from each side. The second device, named "IV," has $L = 3L_c/8, N = 8$ and $b = W_0/8$ (Fig. 1) and the geometrical configuration of Fig. 3 with $W_1/W_0 \approx 0.775$. The inputs are located at $W_0/4$ from each side.

B. Experimental Results on 1×3 Butterfly MMI Couplers

Again, the devices "I" and "II" have been realized in InGaAsP/InP using the waveguide structure of [16] and the dimensions listed in Table 1 for $dW = 0$. The devices have been measured at $\lambda = 1.53 \mu\text{m}$ (Fig. 6). Any splitting ratio with $P_1 = P_3$ can be realized and the devices are polarization insensitive. The excess losses, compared to a straight waveguide, remain lower than 1.0 dB.

V. GENERALIZATIONS OF THE BUTTERFLY CONFIGURATION

In this section we analyze some generalizations of the butterfly design. First, we introduce multisection devices in

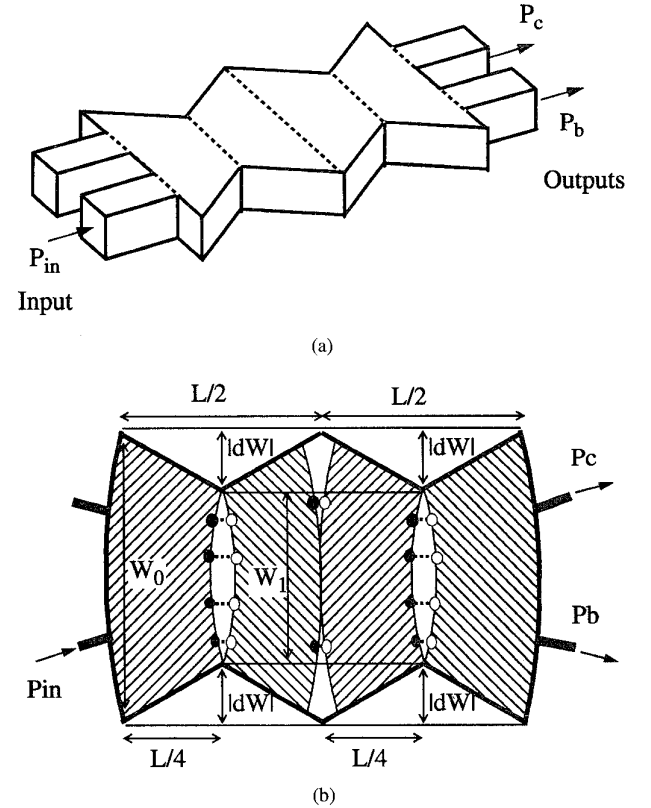


Fig. 7. Symmetrization of the devices "B." Without width variation this new device is identical to the device "B." The new geometrical configuration is fully symmetric and uses a four sections coupler. The length is given by $L = L_c$. The inputs and outputs are located at $W_0/3$ from each side.

order to symmetrize the geometry of the devices "B" and "II." Then we design a mode converter-combiner based on an analog principle as the butterfly geometry. This element has the same functionality as the adiabatic asymmetric Y-junctions.

A. Symmetrical Multisection Devices

The developments made in the previous sections are based on the assumption of a laterally strong guiding waveguide structure. Any deviation from this ideal case leads to a certain amount of radiation, losses, or asymmetry.

In 2×2 splitters, the equal behavior of the two inputs is an important feature. The devices "A" and "C" have a fully symmetrical geometry, even when the widths are varied. The devices "D" can not be symmetrized since the basic element itself is asymmetric, the inputs and outputs being not symmetrically located around the center of the MMI coupler ($x_0 = W_0/5, x_1 = 2W_0/5$ in Fig. 3). In contrast, the asymmetry of the devices "B" are only due to the introduction of the geometrical butterfly transformation of Fig. 4(b). This can be avoided by introducing symmetrical multiple sections in the MMI coupler. Simulations using the mode analysis method have shown that the symmetrical device of Fig. 7 with $L = L_c$ is an advantageous alternative to the device "B." This new device can be interpreted as two devices "A" in series. Without width variation, the device of Fig. 7 is identical to the basic

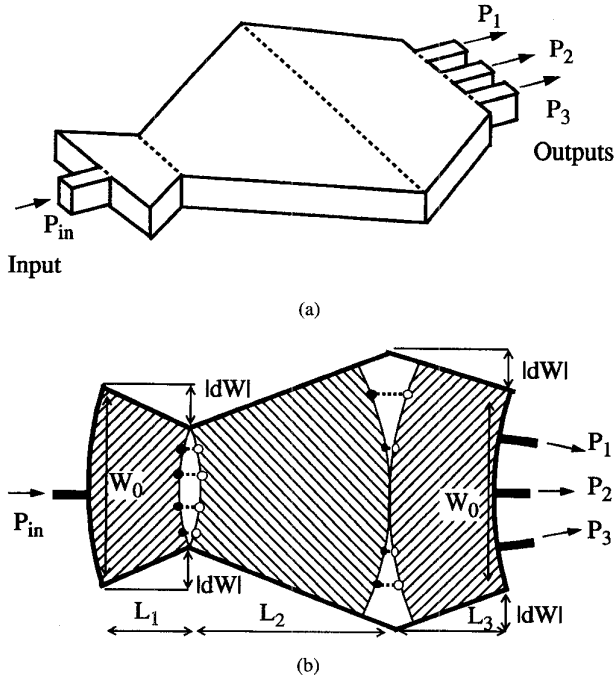


Fig. 8. Symmetrization of the devices "II." Without width variation this new device is identical to the device "II." The new geometrical configuration is fully symmetric and uses a three sections coupler. The lengths are given in the text (8). The input and one output are centered, the two other outputs are located at $W_0/4$ from each side.

device "B," but with width variations the geometry remains symmetric.

For the 1×3 splitters, the two outer outputs should have exactly the same characteristics. For reason of symmetry, this is assured in the devices "I," but not in the devices "II." Simulations show that we can advantageously use the symmetric configuration of Fig. 8 to replace the devices "II." Again, without width variation, this new component and the device "II" are identical. The lengths are given by

$$\begin{aligned} L_1 &\cong n \cdot \frac{W_0 \cdot (W_0 - 2dW)}{4 \cdot \lambda} \\ L_2 &\cong n \cdot \frac{(W_0 - 2dW) \cdot (W_0 + 2dW)}{2 \cdot \lambda} \\ L_3 &\cong n \cdot \frac{W_0 \cdot (W_0 + 2dW)}{4 \cdot \lambda} \end{aligned} \quad (8)$$

and

$$L_3 \cong n \cdot \frac{W_0 \cdot (W_0 + 2dW)}{4 \cdot \lambda}.$$

B. Mode Converter-Combiner Based on MMI Couplers

Not only a width variation dW but also an angle variation $d\alpha$ can produce optical path differences. Based on this idea, a mode converter-combiner can be designed as in Fig. 9. This device images the fundamental mode of the central input I_1 to the fundamental mode of the output O_1 and at the same time it converts the fundamental mode of a second input I_2 to the first order mode of the output O_1 . The angle variation $d\alpha$ is introduced to produce a phase shift of $\pi/2$ between the two outer images after the first section. The width of the input

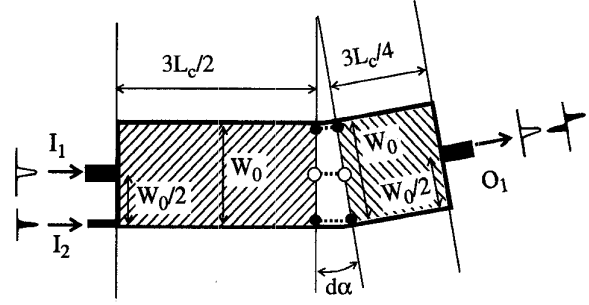


Fig. 9. Design of a mode converter-combiner based on MMI couplers. The fundamental mode of the input I_1 is imaged in the fundamental mode of the output O_1 . The fundamental mode of the input I_2 goes to the first order mode at the output O_1 . The angle variation $d\alpha$ produces a phase shift of $\pi/2$ between the two outer images after the first section.

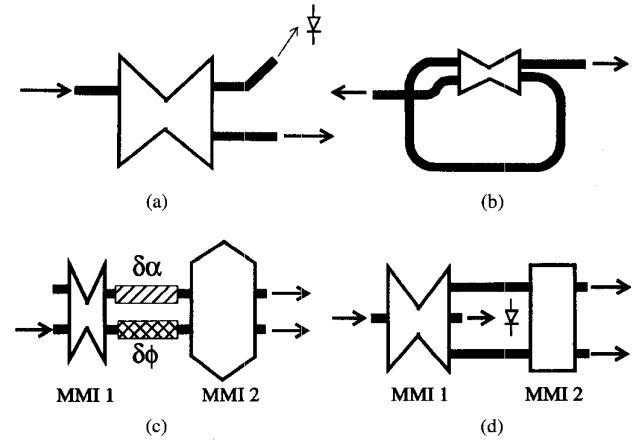


Fig. 10. Applications of the new 2×2 and 1×3 butterfly MMI devices developed in this paper: (a) Tap function: The butterfly element couples out a small part of the light to the photodiode, (b) Ring-lasers: The butterfly MMI coupler controls the quality factor of the optical ring resonator, (c) MZI: A proper choice of the butterfly MMI couplers can compensate for asymmetric loss distribution, (d) Multifunctional device: The 1×3 butterfly MMI couplers act as an output coupler for the monitor photodiode and at the same time as a symmetrical splitter for the MZI.

I_1 and of the output O_1 should be about twice the width of the input I_2 . This device is a compact version of the mode converter-combiner presented in [23].

VI. EXAMPLES OF APPLICATIONS OF THE NEW DEVICES

Some examples of applications of the new devices developed in the previous sections are illustrated in Fig. 10. The "tap" function can be realized with the butterfly 2×2 splitters [Fig. 10(a)]. They are compact, polarization independent, and permit a fine tuning of the outcoupling ratio.

The schematic design of a ring-laser is presented in Fig. 10(b). In order to increase the quality of the resonator, the transmissions to the laser outputs have to be small. This explains the connection of the ring to crossed input-output waveguides. The ease of fabrication and the low losses of MMI couplers have already shown advantages for the realization of ring lasers [9].

Butterfly 2×2 MMI couplers with a free choice of the splitting ratio are also advantageous in Mach-Zehnder interferometers. When the asymmetric losses $\delta\alpha$ are introduced, asymmetric splitting ratios are required to restore a maximum contrast of the interference fringes [Fig. 10(c)]. In switches this improves the on-off ratios. Depending on the relations between the losses $\delta\alpha$ and the phase variations $\delta\phi$, the splitting ratios of both the MMI 1 and MMI 2 should be adapted separately [15]. In this application, the free selection of the splitting ratio and the polarization insensitivity of the butterfly MMI couplers are of relevance.

The 1×3 butterfly devices can work as multifunctional devices as in Fig. 10(d). The monitoring of the signal is assured by the photodiode and at the same time the device acts as a homogeneous power splitter between both arms of the MZI. Note that using the devices "III" or "IV" for this application allow it to have the monitor photodiode at one side. But these devices do not allow it to vary the splitting ratios and simultaneously keep two outputs at equal intensity. The light on the photodiode is fixed at about $1/8$ when the two other outputs are equally illuminated.

As already pointed out, the mode converter-combiner assures the same functionality as a passive adiabatic asymmetric Y-junction. It can therefore find applications in 2×2 digital optical switches [24], in interferometers [25], and in nonlinear all-optical switches [26], [15].

VII. CONCLUSION

A new class of 2×2 and 1×3 MMI couplers has been proposed and realized in InGaAsP/InP. These devices, based on the geometrical butterfly configuration [16], combine a free selection of the splitting ratio with the other advantages of conventional MMI couplers, such as small size, polarization insensitivity, and ease of fabrication. Many different splitting ratios, covering the entire range of possible variations, have been realized. The couplers are polarization-independent and the output powers are accurate within a few percentage points.

The butterfly configuration has been extended to multisection MMI couplers to assure a fully symmetrical geometry and therefore an optimal homogeneity of the device characteristics. Another extension of the butterfly concept has led to the design of a new compact mode converter-combiner.

Some of the interesting applications of these new devices have been briefly analyzed. They cover the topics of optical tap-function, ring-lasers, optical interferometers and switches, nonlinear devices, and multifunctional devices.

REFERENCES

- [1] J. E. Zucker, K. L. Jones, T. H. Chiu, B. Tell, and K. Brown-Goebeler, "Strained quantum wells for polarization-independent electro-optic waveguide switches," *J. Lightwave Technol.*, vol. 10, pp. 1926-1930, 1992.
- [2] M. Bachmann, M. K. Smit, P. A. Besse, E. Gini, H. Melchior, and L. B. Soldano, "Polarization-insensitive low-voltage optical waveguide switch using InGaAsP/InP four-port Mach-Zehnder interferometer," *Tech. Digest OFC/IOOC'93*, San Jose, pp. 32-33, Feb. 21-26, 1993, paper TuH3.
- [3] K. Stubkjaer, T. Durhuus, B. Mikkelesen, C. Joergensen, R. Pedersen, C. Braagaard, M. Vaa, S. Danielsen, P. Doussiere, G. Garabedian, C. Graver, A. Jourdan, J. Jacquet, D. Leclerc, M. Erman, and M. Klenk, "Optical wave length converters," in *Proc. 20th European Conf. Optic. Commun., ECOC'94*, Florence, Sept. 25-29, 1994, pp. 635-642.
- [4] R. Hess, J. Leuthold, J. Eckner, C. Holtmann, and H. Melchior, "All-optical space switch featuring monolithic InP-waveguide semiconductor optical amplifier interferometer," *Optical Amplifiers and Their Applications*, vol. 18, 1995, OSA Technical Digest Series, Optical Society of America, Washington, DC, 1995, paper PD2.
- [5] O. Bryngdahl, "Image formation using self-imaging techniques," *J. Opt. Soc. Amer.*, vol. 63, pp. 416-419, 1973.
- [6] R. Ulrich and T. Kamiya, "Resolution of self-images in planar optical waveguides," *J. Opt. Soc. Amer.*, vol. 68, no. 5, pp. 583-592, 1978.
- [7] L. Soldano, F. Veerman, M. Smit, B. Verbeek, A. Dubost, and E. Pennings, "Planar monomode optical couplers based on multimode interference effects," *J. Lightwave Technol.*, vol. 10, pp. 1843-1849, Dec. 1992.
- [8] J. M. Heaton, R. M. Jenkins, D. R. Wight, J. T. Parker, J. C. H. Birbeck, and K. P. Hilton, "Novel 1-to-N way integrated optical beam splitters using symmetric mode mixing in GaAs/AlGaAs multimode waveguides," *Appl. Phys. Lett.*, vol. 61, no. 15, pp. 1754-1756, 1992.
- [9] L. Soldano and E. Pennings, "Optical multi-mode interference devices based on self-imaging: Principles and applications," *J. Lightwave Technol.*, vol. 13, pp. 615-627, Apr. 1995.
- [10] M. Bachmann, "Polarization insensitive integrated optical waveguide switches using InGaAsP/InP," *Ph.D. thesis, diss. ETHZ-Zurich no. 11072*, Switzerland, 1995.
- [11] P. A. Besse, M. Bachmann, H. Melchior, L. B. Soldano, and M. K. Smit, "Optical bandwidth and fabrication tolerances of multimode interference couplers," *J. Lightwave Technol.*, vol. 12, pp. 1004-1009, 1994.
- [12] M. Bachmann, P. A. Besse, and H. Melchior, "General self-imaging properties in $N \times N$ multimode interference couplers including phase relations," *Applied Optics*, Vol. 33, pp. 3905-3911, July 1994.
- [13] ———, "Overlapping-image multi-mode interference couplers with reduced number of self-images for uniform and nonuniform power splitting," *Appl. Opt.*, vol. 34, no. 30, pp. 6898-6910, Oct. 1995.
- [14] R. van Roijen, E. C. M. Pennings, M. J. N. van Stralen, T. van Dongen, B. H. Verbeek, and J. M. M. van der Keijden, "Compact InP-based ring lasers employing multimode interference couplers and combiners," *Appl. Phys. Lett.*, vol. 64, pp. 1753-1755, 1994.
- [15] J. Leuthold and P. A. Besse, "Kompakte optisch-optische schalter und wellenlängen-konverter mittels multimode-interferenz modekonvertern," *Patent Application PCT/CH96/00035*, vol. 29, Jan. 1996.
- [16] P. A. Besse, E. Gini, M. Bachmann, and H. Melchior, "New 1×2 multimode interference couplers with free selection of power splitting ratios," in *Proc. 20th European Conf. Optic. Commun., ECOC'94*, Florence, Sept. 25-29, 1994, pp. 669-672.
- [17] W. Burns and F. Milton, "Mode conversion in planar-dielectric separating waveguides," *IEEE J. Quantum Electron.*, vol. QE-11, pp. 32-39, Jan. 1975.
- [18] M. Bachmann, Ch. Nadler, P. A. Besse, and H. Melchior, "Compact polarization-insensitive multi-leg 1×4 mach-zehnder switch in InGaAsP/InP," *ECOC'94*, Firenze, Sept. 25-29, 1994.
- [19] R. Ulrich and G. Ankele, "Self-imaging in homogeneous planar optical waveguide," *Appl. Phys. Lett.*, vol. 27, no. 6, pp. 337-339, 1975.
- [20] P. A. Besse, "Method of changing the intensity and phase distribution in multimode interference couplers," USA, Canada, Patent Application PHQ 93.027 US/CA, July 1995.
- [21] P. Besse, M. Bachmann, and H. Melchior, "Phase relations in multimode interference couplers and their application to generalized integrated Mach-Zehnder optical switches," in *Proc. ECIO 93*, Neuchatel, paper 2-22.
- [22] P. A. Besse, M. Bachmann, C. Nadler, and H. Melchior, "The integrated prism interpretation of multi-leg Mach-Zehnder interferometers based on multimode interference couplers," *Optic. Quantum Electron.*, vol. 27, pp. 909-920, 1995.
- [23] R. Hess, J. Leuthold, P. A. Besse, and H. Melchior, "Optical mode-combiners based on planar multi-mode interference couplers in InGaAsP/InP," in *Proc. ECIO'95*, Delft, The Netherlands, Apr. 1995, paper WeA3, 3.-6., pp. 327-330.
- [24] Y. Silberberg, P. Perlmuter, and J. Baran, "Digital Optical Switch," *Appl. Phys. Lett.*, vol. 51, pp. 1230-1232, Oct. 1987.
- [25] W. Burns and F. Milton, "An analytic solution for mode coupling in optical waveguide branches," *IEEE J. Quantum Electron.*, vol. QE-16, pp. 446-454, Apr. 1980.
- [26] G. J. M. Krijnen, A. Villeneuve, G. Stegeman, S. Aitchison, P. Lambeck, and H. Hoekstra, "Modeling of a versatile all-optical Mach-Zehnder Switch," in *Int. Symp. Guided-Wave Optoelectron., Weber Research Institute*, Brooklyn, USA, Oct. 26-28, 1994, paper VII.6.



Pierre A. Besse was born in Sion, Switzerland, in 1961. He received the degree in physics and his Ph.D. degree in semiconductor optical amplifiers from the Swiss Federal Institute of Technology, ETH Zurich, in 1986 and 1992, respectively.

In 1986, he joined the group of micro- and optoelectronics at the Institute of Quantum Electronics in ETH Zurich, where he is engaged in research on optical telecommunication science. He worked on theory, modeling, characterization, and fabrication of compound semiconductor devices such

as polarization-independent optical switches and modulators, passive optical components such as star couplers, multimode interference couplers and wavelength demultiplexers on III-V materials, as well as polarization-independent traveling wave semiconductor optical amplifiers and external cavity tunable laser sources. In August 1994, he joined the Department of Microengineering at the Swiss Federal Institute of Technology at Lausanne (EPFL) as Senior Assistant, where he is involved with activities on sensors and actuator microsystems. His major fields of interest are physical principles and new phenomena for optical, magnetical, inductive, and strain sensors. He is also interested in design activities in all-optical switches and gain-clamped semiconductor optical amplifiers. He has been involved in international projects such as the RACE/OSCAR and ATMOS projects of the European Community. He is involved in the Swiss Priority Program MINAST on micro and nano structures. He has written and coauthored more than 40 scientific papers and conference contributions. He holds eight patent applications.



Emilio Gini was born in Davos, Switzerland, on September 20, 1961. He received the degree in physics from the Swiss Federal Institute of Technology in 1986.

He joined the Institute of Quantum Electronics in 1988. He worked on the growth of III-V compounds by LP-MOVPE and dry etching techniques for the fabrication of optoelectronic integrated circuits (OEIC's). He participated in different European RACE, ESPRIT, and COST projects where he was involved in the development of low-loss

optical waveguides with integrated corner mirrors and polarization-insensitive optical switches and modulators. His current interests concentrate on the design, fabrication, and characterization of InP-based optical demultiplexers for multiwavelength transmission systems. He has written and coauthored more than ten scientific papers and conference contributions.



Maurus Bachmann was born in Grabs, Switzerland, in 1961. He studied at the Swiss Federal Institute of Technology, ETH Zurich, where he received the degree in physics in 1986 and the Ph.D. degree in polarization-insensitive optical waveguide switches in 1995.

In 1986, he joined the Micro- and Optoelectronics Group of the Institute of Quantum Electronics, ETH Zurich, where he has been involved in international projects such as RACE/OSCAR and RACE/ATMOS of the European Community. His main areas of

research involve theory, design, fabrication, and characterization techniques of InGaAsP/InP-based integrated optical components for telecommunications applications. His major fields of interest are polarization-insensitive optical switches and modulators, as well as passive integrated optical components like multimode interference couplers. Recently, he joined Alcatel Alsthom Recherche, Marcoussis, France, where he is engaged in research on integrated optical devices.



Hans Melchior (S'62-M'65-SM'80-F'95) received the Dipl. El.-Ing. and the Dr. Sc. Techn. degrees from the Swiss Federal Institute of Technology, Zurich, Switzerland, in 1959 and 1965, respectively. His dissertation covered the dynamics and noise characteristics of *p-n* junctions in breakdown and of tunnel diodes. He also did early work on the second breakdown of transistors.

From 1965 to 1976 he worked at Bell Telephone Laboratories, Murray Hill, NJ. He developed germanium and silicon avalanche photodiodes and realized photodiodes with response times below 50 ps. He was then involved in the investigation and development of photoconductors and ferroelectric and liquid crystal light valve displays. Starting in 1970, he participated in the development of fiber-optical communication and developed silicon avalanche photodiodes for the first fiber optical trials in Atlanta, GA. In 1976 he joined the Swiss Federal Institute of Technology, Zurich, as Professor of electronics, initially responsible for silicon technology, CMOS-integrated circuits, and optoelectronics. His present interests include semiconductor lasers, optical waveguide switches, and high-speed optoelectronic components, as well as compound semiconductors technology for their realization and the applications in fiber-optical communication and picosecond optoelectronics. From 1979 to 1986, he also served as Director of a group doing industry-orientated research and development. From 1984 to 1986, he was Dean of the Department of Electrical Engineering. He participated in organizing committees of scientific conferences, including ECOC, microcircuit engineering, and semiconductor laser conference. From 1984 to 1986, he was Associate Editor of the JOURNAL OF LIGHTWAVE TECHNOLOGY.

Dr. Melchior is a member of the Swiss Academy of Engineering Sciences. He was the recipient of the 1990 GEP Prize for efforts toward European research.